An Observational Test of Transition Region Lines as a Pressure Gauge

N. W. Griffiths[1], G. H. Fisher and O. H. W. Siegmund[1]

Space Sciences Laboratory, University of California, Berkeley, CA 94720

Abstract.

We report on observations of solar transition region lines made with the SUMER instrument on SOHO. The use of such lines as a pressure gauge is investigated. The observed N V fluxes and the distribution of intensity in the different lines are also discussed.

1. Introduction

The simplest models of the chromosphere-corona transition region assume a balance between the divergence of conductive heat flux and optically thin radiative losses. Hawley and Fisher (1992) used this assumption to derive numerical proportionalities between the plasma pressure at 10^5K and the surface flux of transition region lines such as CIV (1548Å) and NV (1242Å). While it is generally thought that this model is too simple to explain observed emission measure distributions below 10^5K, it would be interesting to see if the model applies at *any* transition region temperature.

2. Theory

It is straightforward to derive the "pressure gauge" relationship using standard expressions for the conductivity (Spitzer 1962) and radiative losses:

$$F_c = -\kappa_0 \, T_e^{5/2} \, \frac{dT_e}{dz} \tag{1}$$

$$\nabla.\mathbf{F_r} = N_e \, N_H \, \Lambda(T_e). \tag{2}$$

Equating conduction and radiative losses

$$\nabla.\mathbf{F_c} = -\nabla.\mathbf{F_r} \tag{3}$$

$$\frac{dF_c}{dz} = -N_e \, N_H \, \Lambda(T_e) \tag{4}$$

[1]Experimental Astrophysics Group

$$F_c \frac{dF_c}{dz} = -N_e\, N_H\, \Lambda(T_e)\, F_c \tag{5}$$

$$\frac{d}{dz}(F_c^2) = 2\, N_e\, N_H\, \Lambda(T_e)\, \kappa_0\, T_e^{5/2}\, \frac{dT_e}{dz}. \tag{6}$$

By defining $X = N_H/N_e$ we can write

$$dF_c^2 = 2X\, \frac{P_e^2}{k_B^2 T_e^2}\, \Lambda(T_e)\, \kappa_0\, T_e^{5/2}\, dT_e \tag{7}$$

$$F_c^2 = 2X\, \frac{P_e^2}{k_B^2}\, \kappa_0 \int_{T_0}^{T_1} \Lambda(T_e)\, T_e^{1/2}\, dT_e. \tag{8}$$

Now, let us define $\lambda(T_e)$ to be

$$\lambda(T_e) = \int_{T_0}^{T_1} \Lambda(T_e)\, T_e^{1/2}\, dT_e. \tag{9}$$

Therefore

$$F_c = \sqrt{2X\kappa_0}\, \frac{P_e}{k_B} \lambda^{1/2}(T_e). \tag{10}$$

The power in an emission line can be written as

$$E_{\star ji} = 8.6 \times 10^{-6} \frac{hc}{\lambda} \frac{\Omega_{ij}}{\omega_i} \frac{N_E}{N_H} \int \frac{N_i}{N_{ion}} N_e N_H\, g(T_e)\, A\, dz \tag{11}$$

where A is the area of the plane parallel atmosphere over which the flux is being formed. We can rewrite this as

$$E_{\star ji} = \int G(T_e)\, A\, N_e N_H\, dz \tag{12}$$

where $G(T_e) = 8.6 \times 10^{-6} \frac{hc}{\lambda} \frac{\Omega_{ij}}{\omega_i} \frac{N_E}{N_H} \frac{N_i}{N_{ion}}\, g(T_e)$.
Using (1), we can write

$$dz = -\frac{\kappa_0\, T_e^{5/2}\, dT_e}{F_c}. \tag{13}$$

Therefore, since the observed flux $F_\star = E_{\star ji}/2A$

$$F_\star = P_g \int \frac{1}{4} \sqrt{\left(\frac{X\kappa_0}{2}\right)}\, \frac{G(T_e)\, T_e^{1/2}\, dT_e}{k_B \lambda^{1/2}(T_e)} \tag{14}$$

i.e.

$$F_\star = P_g\, \alpha \tag{15}$$

where α is the integral of the temperature dependent terms.

Since the thickness of the solar atmosphere in the temperature range $4.0 \leq \log T_e \leq 5.7$ is only ~ 100 km, we should expect the pressure in the transition region to be essentially uniform. Consequently, if this simple model *is* correct, the ratio of observed flux to α should be constant and independent of the chosen line.

3. SUMER Observations

The high spatial and spectral resolution of the SUMER instrument (Wilhelm et al. 1995) allows us to investigate the solar transition region very accurately, and we have designed observing sequences to study the "pressure gauge" relationship derived above. Our observations include lines from N II, N III, N IV and N V, formed over the temperature range $4.4 \leq \log T_e \leq 5.3$, and lines from O II, O III, O IV and O V which are formed in a similar temperature range. We can isolate the role of possible abundance variations by examining lines from each element separately. In addition, we also observed the O IV density sensitive multiplet at 1400 Å to obtain an independent measure of the transition region pressure.

Table 1. Observed Transition Region Lines.

Nitrogen Lines			*Oxygen Lines*		
Ion	**log T_e**	λ(Å)	**Ion**	**log T_e**	λ(Å)
N II	4.4	776.0	O II	4.5	833.3, 834.5
N III	4.9	764.4	O III	5.0	833.7
N IV	5.1	765.1	O IV	5.2	787.7
N V	5.3	1238.8, 1242.8	O IV	5.2	1399.8, 1401.2, 1404.8, 1407.4
			O V	5.4	760.4

Since the raster mechanism on SUMER has been disabled, our observations were taken with the slit fixed at disk center and the Sun rotating through our field of view. The lines were split up into 4 wavelength bands, and each band was subject to multiple 60 s exposures. We made observations of both the quiet Sun and active regions. Here we review results from an 8 hour quiet Sun observation, made using the $1 \times 300\,\mathrm{arcsec}^2$ slit.

4. Data Reduction

The SUMER detectors are microchannel plate arrays, electronically digitized to 1024 (spectral) $\times$ 360 (spatial) pixels. A distortion of the detector grid exists on the pixel scale, and the optics lead to a wavelength dependence in the size of the slit on the detector. In our observations we are mainly concerned with

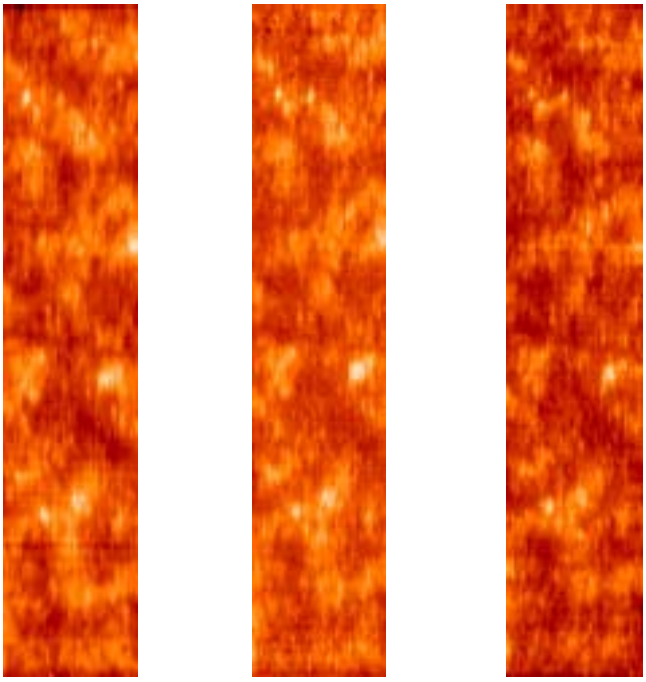

Figure 1. SUMER Intensity Maps.
From left to right : N V 1238.8Å, O IV 1401.2Å and O III 833.7Å.

line fluxes integrated over the whole line profile, so the small scale distortion is not important. However, we do want to compare spectroheliograms from lines at different wavelengths, so all exposures were normalised to 300 arcsec in the spatial direction.

The flat-field correction was completed manually, and no data compression was used in the telemetry in order to minimise losses. Each line profile was studied as a function of time, so that the position of the line on the detector and the level of the background could be accurately determined for each emission feature.

5. Results

5.1. Intensity Maps

The time between each exposure of a given line is about 6.7 minutes. This is close to the time it would take the Sun to rotate by 1 arcsec perpendicular to the SUMER slit. Therefore, even though the raster mechanism is disabled, we can still build up spectroheliograms that are very close to the correct aspect ratio.

In Figure 1 we show intensity maps for the N V 1238.8Å, O IV 1401.2Å and O III 833.7Å lines, formed at temperatures of $\sim 2 \times 10^5$ K, $\sim 1.5 \times 10^5$ K and $\sim 1 \times 10^5$ K respectively.

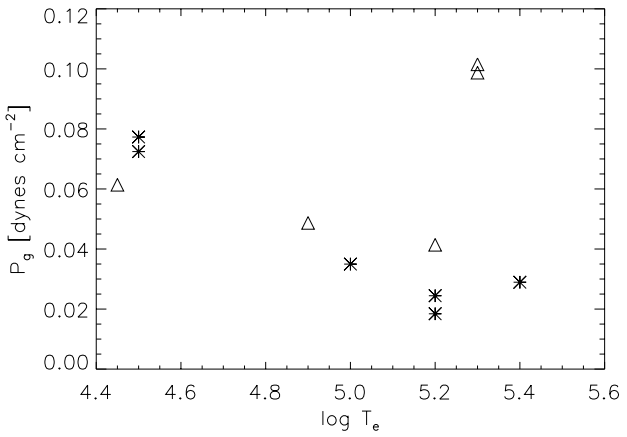

Figure 2. Results over entire Field of View.

$\triangle$ = Nitrogen lines, $*$ = Oxygen lines.

5.2. Transition Region Pressure

Our observations included measurements of the O IV multiplet at 1400Å. Ratios of lines in this multiplet can theoretically yield values for the electron density (Cook et al. 1995, Brage et al. 1996). In practice there are problems associated with two of these lines. The 1404.8Å line is blended with a line of S IV, and in SUMER spectra the 1407.4Å line is blended with the O III 703.9Å line in second order. We therefore prefer to estimate the pressure using the 1399.8Å/1401.2Å ratio.

Averaged over the whole observation the value of this line ratio is 0.184±7%. Using the results of Cook et al. (1995), this corresponds to an electron density of $\log N_e = 9.63^{+0.26}_{-0.54}$. The uncertainties are large because in this regime N_e is a very rapidly changing function of the line ratio.

The O III second order blend with the O IV 1407.4Å profile can be estimated from the observed O III 833.7Å flux. Using this estimate the 1407.4Å/1401.2Å ratio predicts a density of $\log N_e = 9.71$. This agrees well with the previous value, but the uncertainties are likely to be even larger.

5.3. Pressure Gauge Results

By comparing the observed flux and the pressure gauge parameter α for each line we can determine values for the gas pressure P_g. These values are shown in Figure 2. We see that they are all somewhat smaller than the value of 0.18 dynes cm^{-2} determined from the O IV line ratio. The N V emission is much stronger than expected, and this is discussed in §5.5.

5.4. Differential Emission Measure Distributions

We can use the measured plasma pressure to determine the DEM distribution predicted by the "pressure gauge" theory:

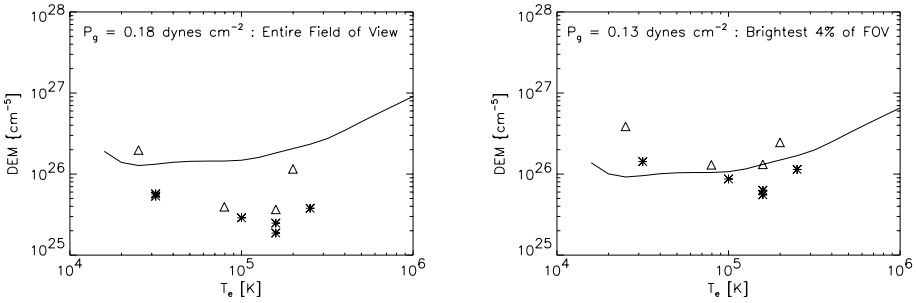

Figure 3. Solid line = "Pressure Gauge" DEM.
$\triangle$ = DEM from Nitrogen lines, $*$ = DEM from Oxygen lines.

$$\xi(T) = N_e^2 \frac{T_e}{|dT/dz|} = \frac{P_g}{k_B} \sqrt{\frac{\kappa_0}{8X}} \frac{T_e^{3/2}}{\lambda^{1/2}(T_e)} \tag{16}$$

This can be compared to DEM values determined from individual emission lines, as shown in Figure 3. We see that over the entire field of view the "pressure gauge" DEM compares very poorly with the individual points. However, when we confine our attention to the brightest 4% of the FOV (corresponding to $\simeq$ 15% of the total flux in N IV), the O IV line ratio predicts an electron pressure of $\log N_e \sim 9.5$, and the agreement between the "pressure gauge" DEM and the individual points is much better.

5.5. N V Fluxes

As mentioned above, the N V 1240Å emission is much stronger than expected (by a factor of $\sim$ 2.4). Figure 4 indicates that this effect may become less pronounced at high intensity.

Higher than predicted line intensities for the Li and Na isoelectronic sequences have been observed on a number of occasions (e.g. Dupree 1972, Judge et al. 1995). Dynamical processes are known to affect these line intensities (e.g. Hansteen 1993), and may go some way to explaining the discrepancy. Another source of error is the omission of density dependence in di-electronic recombination from some ionization equilibrium calculations, such as those of Arnaud and Rothenflug (1985) which we adopt here. As demonstrated by Jordan (1969), the inclusion of di-electronic recombination in the ionization equilibria of these sequences can significantly alter the line intensities.

5.6. Distribution of Line Intensity

Figure 5 indicates that the pixel brightness for N IV 765.1Å is log-normally distributed. We find that similar distributions exist for all the lines observed in this study. This may suggest that the emission is associated with small, fragmenting magnetic elements (Bogdan et al. 1988, Berger et al. 1995).

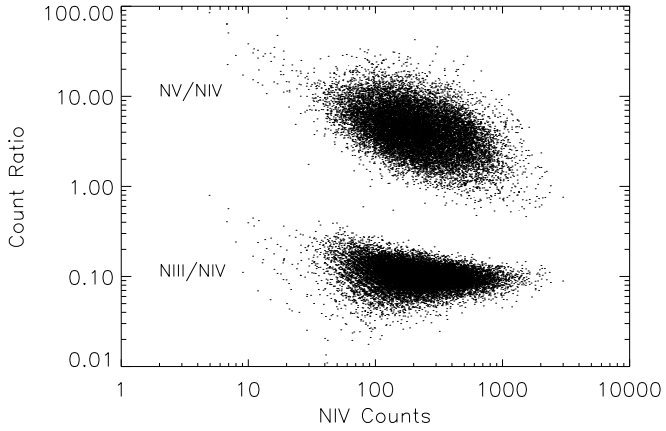

Figure 4. N V/N IV and N III/N IV line ratios as a function of N IV intensity.

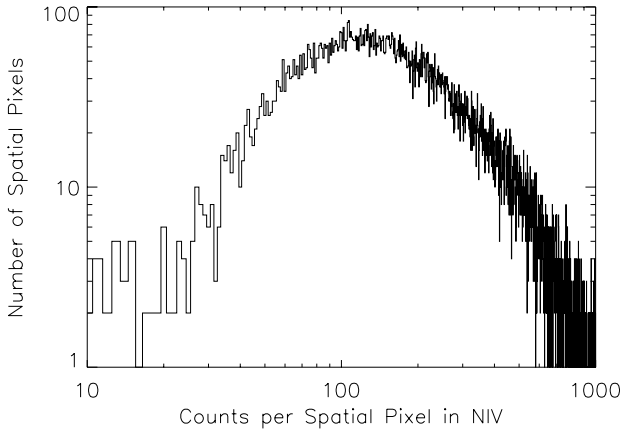

Figure 5. Distribution of Pixel Brightness.

6. Conclusions

We suggest the following preliminary conclusions:

• The "pressure gauge" approach appears to fail at all transition region temperatures when we consider unresolved data from an extended portion of the quiet Sun.

• When we consider only the brightest pixels, we find that the "pressure gauge" may apply above $\sim 10^5$ K. To test this possibility we will use our data to compare conduction and radiative losses across the transition region. If conduction and radiation do not balance then the model is not valid and any apparent agreement with the observations must be explained another way. We note that Jordan et al. (1987) studied IUE data for five G-K dwarfs, and found empirical evidence for an almost linear relationship between pressure and intensity of the Si IV, C IV and N V lines. The Si IV and (possibly) the C IV lines are formed at a temperatures where conduction and radiation are unlikely to balance. The almost linear dependence on pressure may therefore be the result of an alternative mechanism.

• We observe higher than expected emission in N V, confirming earlier results. However, there is evidence to suggest that this effect may diminish at high intensities.

• All the line intensities appear to be log-normally distributed, indicating the possible presence of magnetic fragmentation.

Acknowledgments. The authors wish to thank Giampiero Naletto, Tod Woods, Phil Judge and Carole Jordan for their helpful discussions.

This work was supported by NASA.

References

Arnaud, M., & Rothenflug, R. 1985, A&AS, 60, 425

Berger, T. E., Schrijver, C. J., Shine, R. A., Tarbell, T. D., Title, A. M., & Scharmer, G. 1996, ApJ, 454, 531

Bogdan, T. J., Gilman, P. A., Lerche, I., & Howard, R, 1988, ApJ, 327, 451

Brage, T., Judge, P. G., & Brekke, P. 1996, ApJ, 464, 1030

Cook, J. W., Keenan, F. P., Dufton, P. L., Kingston, A. E., Pradhan, A. K., Zhang, H. L., Doyle, J. G., & Hayes, M. A. 1995, ApJ, 444, 936

Dupree, A. K. 1972, ApJ, 178, 527

Hansteen, V., 1993, ApJ, 402, 741

Hawley, S. L., & Fisher, G. H. 1992, ApJS, 78, 565

Jordan, C. 1969, MNRAS, 142, 501

Jordan, C., Ayres, T. R., Brown, A., Linsky, J. L., & Simon, T. 1987, MNRAS, 225, 903

Judge, P. G., Woods, T. N., Brekke, P., & Rottmann, G. J. 1995, ApJ, 455, L85

Spitzer, L. 1962, in Physics of Fully Ionized Gases (New York:Interscience)

Wilhelm, K., et al. 1995, Solar Phys., 162, 189